IEEE Transactions on Robotics (T-RO) paper, presented at ICRA 2023, London, UK. Cite as T-RO paper.

Kinematic Redundancy Analysis for (2n+1)R Circular Manipulators

Zijia Li, Mathias Brandstötter, and Michael Hofbaur

***Abstract*—The kinematic analysis of redundant serial manipulators with $2n+1$ revolute joints (integer $n \geq 3$), which we call circular manipulators, is presented in this paper. The structure of the kinematic chain of circular manipulators has special properties that can be seen in the Denavit-Hartenberg parameters: all orthogonal distances are zero, all even-numbered offsets are zeros, but odd-numbered offsets are not. Typical manipulators that fulfill these properties are redundant 7R serial chains ($n = 3$) that mimic the human arm, e.g., the lightweight robot arm KUKA LBR iiwa. This 7R circular manipulator has self-motion as rotation around an axis that goes through two fixed points for a fixed pose. First, radical reparametrization is presented based on the swivel angle of the closed-form inverse kinematics solution for the 7R circular manipulator. Second, for a six-dimensional task, the inverse kinematics solution for redundant serial manipulators with $2n+1$ revolute joints ($n \geq 3$) is reparametrized by the swivel angle and other $2n-6$ rotation parameters. From a geometric point of view, for a circular manipulator with $2n+1$ revolute joints, one can have $n(n-1)/2$ choices of such circular rotations. Third, we conjecture numerical kinematic singularities for circular manipulators in a recursive formula, confirming $n = 5, 6, 7$.**

***Index Terms*—Redundant Robots, Kinematic Singularities, Industrial Robots, Collision Avoidance, recursively solution**

I. Introduction

Nowadays, robots, especially serial manipulators like anthropomorphic redundancy manipulators, which have a spherical wrist (the last three rotational axes intersect at one point), are well-implemented in industry and well-studied [1], [2], [3], [4], [5], [6]. By symmetry, one can build a manipulator such that the first three revolute joints intersect at one point called the shoulder point. One well-known manipulator that came up with this idea is the KUKA LBR iiwa (see Fig. 1a), which has seven revolute joints. An additional joint called the elbow connects its wrist and shoulder and is an intersection point of three rotational axes. From a geometric point of view, we have three important points for the KUKA LBR iiwa: the shoulder point P_s, the elbow point P_b, and the wrist point P_w.

We can extend these manipulators with such three points to a manipulator with n points for (integer $n \geq 3$). It can be done by continuously adding two more joints at the current end such that the last three axes form a wrist/shoulder again. For simplicity, in this paper, we let all twist angles α be ± 90 degree (one could consider cases with other twist angles similarly). We call serial manipulators with such a structure *circular manipulators*. More precisely, they are defined to have all orthogonal distances equal to zero, and all even-numbered offsets are zeros. However, odd-numbered offsets are nonzero regarding standard Denavit-Hartenberg parameters [7]. As a consequence, we can parameterize the inverse kinematics solution by rotations. Following these rotations, the *circular* comes from the fact that every elbow traces a circle around the adjacent shoulder and wrist joints.

Although the closed-form inverse kinematics solution of the KUKA LBR iiwa (7R) is well studied in the literature [1], [5], [8] and recently some novel results as [9], [10], [11], interesting properties have emerged from our analysis. Our first novel contribution is a re-parametrization of the closed-form solution for 7R circular manipulators using the swivel angle. This re-parametrization contains a closed formula for all angles and hence gives us the possibility to calculate the rotational angles in parallel; namely, we solve the orientation inverse procedure in advance (instead of solving it after we know partial rotation angles as in [2], [5], [9], [10]). This paper appears to be the first to simultaneously solve the closed-form solution for the wrist and shoulder. Furthermore, we give a clear pattern for the relations of the eight copies of the circle described by the elbow, which appears to be new compared to [10].

In redundant serial manipulators' kinematic analysis, the null space method is well studied and used in the literature, e.g., to minimize joint displacements [12], avoid obstacles [13], task-priority based redundancy control [14], minimize kinetic energy [15] and optimize joint torques [16]. More recent works involve a generalized framework for multiple task management [17], and problems with joint saturation [18], [19]. For optimization and general issues regarding the redundancy analysis, we refer to the seminal work of Nakamura [20]. One of the most significant advantages of using the null-space method is that the control strategies can be made following different decomposition of the null space.

Notice that the most significant advantage of these serial manipulators is that their inverse kinematics and kinematic singularities are easily computed [1], [2], [5]. Also, because of the success of the KUKA LBR iiwa, they have many applications in the industry nowadays. On the other hand, one of its disadvantages might be that they have lots of kinematic singularities, which reduces the workspace when the null space method is used.

Z. Li is with the KLMM, Academy of Mathematics and Systems Science, Chinese Academy of Sciences, Beijing 100190, China e-mail: lizijia@amss.ac.cn.

M. Brandstötter and M. Hofbaur are with JOANNEUM RESEARCH, Institute for Robotics and Mechatronics, Lakeside B13b, 9020 Klagenfurt am Wörthersee, Austria, email: {mathias.brandstoetter, michael.hofbaur}@joanneum.at. Additionally, M. Hofbaur is with Alpen-Adria Universität Klagenfurt, Department of Smart Sensor Technologies, 9020 Klagenfurt am Wörthersee, Austria

Corresponding author: Z. Li (email: lizijia@amss.ac.cn).

IEEE Transactions on Robotics (T-RO) paper, presented at ICRA 2023, London, UK. Cite as T-RO paper.

Another novel contribution is a general inverse kinematics solution for $(2n{+}1)$R circular manipulators based on this re-parametrization. The 9 DoF circular manipulator built by Schunk modules (Schunk 9R manipulator) is analyzed by this re-parametrization method. A general framework for solving the inverse kinematics problem of a serial manipulator can be obtained by the automatic inverse kinematics solution [21]. Here we focus on a particular pattern; namely, we use the sub-chain with the inverse kinematics solution of the 7R circular manipulators. The swivel angle and $2n$-6 additional rotation parameters are used to solve the inverse kinematics problem. From the geometric point of view, the solution corresponds to a rotation around an axis that goes through two center points where three adjacent axes intersect (excluding directly adjacent center points). For a $(2n{+}1)$R circular manipulator, there are exact n center points for the manipulator. The number $\binom{n}{2} - (n-1) = \frac{(n-1)(n-2)}{2}$ for integer $n \geq 3$ gives us the possibility to choose many 1-DoF closed-form solutions from the high-dimensional inverse kinematic solution of a $(2n{+}1)$R circular manipulator. Using this decomposition, we can also develop more control strategies like the null space method. The superiority is that we have proper forms compared to the numerical null space method.

Kinematic singularities studies are also essential for mechanisms and manipulators, see [22]. This paper shows the computation of kinematic singularity varieties for circular manipulators. We can compute the intersection of their corresponding varieties using the prime decomposition. Based on the particular shape of the circular manipulators, we conjecture a recursive procedure to obtain the singularities varieties of a $(2n{+}1)$R circular manipulator, and the conjecture confirms when $n = 5, 6, 7$ using Gröbner Basis.

The remaining part of the paper is set up as follows. In Section II, the elementary preparations for the paper, where 4×4 matrices combining Denavit-Hartenberg parameters for the forward kinematics equations are introduced. In Section III, a re-parametrization of the inverse kinematics for 7R circular manipulators, using shoulder solution, elbow solution, wrist solution, and swivel angle is shown. In Section IV, we give an (closed-form) inverse kinematics solution for $(2n{+}1)$R circular manipulators. In Section IV-B, we reveal the geometric representations of the inverse kinematics solution for circular manipulators. In Section V, we give a formula for the kinematic singularities of $(2n{+}1)$R circular manipulators. A summary of our results and a prospect for control strategies will be presented in Section VI.

II. Elementary preparations

The following elementary preparations serve the understanding of the subsequent chapters.

A. Geometry of circular manipulators

In order to obtain the kinematic model, we use the standard geometric parameters in the Denavit-Hartenberg convention [7]. However, with different choices (orientation of lines) for locating the coordinate axes, we will only list one choice of numerical Denavit-Hartenberg parameters in Tab. I.

i-th Link	a_i	d_i (mm)	α_i	θ_i
1	0	d_1	90	θ_1
2	0	0	-90	θ_2
3	0	d_3	90	θ_3
4	0	0	-90	θ_4
$\vdots$	$\vdots$	$\vdots$	$\vdots$	$\vdots$
$2n-1$	0	d_{2n-1}	90	θ_{2n-1}
$2n$	0	0	-90	θ_{2n}
$2n+1$	0	d_{2n+1}	0	θ_{2n+1}

TABLE I: Denavit-Hartenberg geometric parameter assignment of $(2n{+}1)$R circular manipulators.

Fig. 1 shows a KUKA LBR iiwa 7R manipulator and a Schunk 9R manipulator. For KUKA LBR iiwa 7, we have $d_1 = 0.340\,\text{m}$, $d_3 = 0.400\,\text{m}$, $d_5 = 0.400\,\text{m}$, $d_7 = 0.126\,\text{m}$. For KUKA LBR iiwa 14, we have $d_1 = 0.360\,\text{m}$, $d_3 = 0.420\,\text{m}$, $d_5 = 0.400\,\text{m}$, $d_7 = 0.126\,\text{m}$. For the geometric invariant parameters of the Schunk 9 DoF, we have $d_1 = 0.380\,\text{m}$, $d_3 = 0.360\,\text{m}$, $d_5 = 0.328\,\text{m}$, $d_7 = 0.323\,\text{m}$, $d_9 = 0.0824\,\text{m}$.

B. Matrix Notations

In kinematics, the 4×4 homogeneous transformation matrices are widely used for describing the special Euclidean group $\mathrm{SE}(3)$, i.e., the group of maps from $\mathbb{R}^3$ to itself that preserve Euclidean distances and orientation. We follow the construction of the homogeneous transformation matrices from [5]. Let $\mathbf{M}$ be a 4×4 matrix

$$\mathbf{M} := \begin{pmatrix} 1 & \mathbf{0} \\ \mathbf{p} & \mathbf{R} \end{pmatrix},$$

where $\mathbf{p}$ is a vector in $\mathbb{R}^3$ and $\mathbf{R}$ is a 3×3 orthogonal matrix of determinant 1. For instance, the subgroup of rotations around the z-axis can be parametrized as

$$\mathbf{M}(\theta) = \begin{pmatrix} 1 & 0 & 0 & 0 \\ 0 & \cos(\theta) & -\sin(\theta) & 0 \\ 0 & \sin(\theta) & \cos(\theta) & 0 \\ 0 & 0 & 0 & 1 \end{pmatrix}, \qquad (1)$$

where θ is the rotational angle. By introducing $t := \tan\left(\frac{\theta}{2}\right)$ the rotational matrix in Eq. (1) can be reparametrized with the parameter t (tangent half-angle substitution) as

$$\mathbf{M}(t) = \begin{pmatrix} 1 & 0 & 0 & 0 \\ 0 & \frac{1-t^2}{1+t^2} & -\frac{2t}{1+t^2} & 0 \\ 0 & \frac{2t}{1+t^2} & \frac{1-t^2}{1+t^2} & 0 \\ 0 & 0 & 0 & 1 \end{pmatrix}.$$

Using the Denavit-Hartenberg parameter convention, the forward kinematics for $(2n{+}1)$R circular manipulators can be written down as

$$\mathbf{M}_e = \mathbf{M}_1(t_1)\mathbf{G}_1\mathbf{M}_2(t_2)\cdots\mathbf{M}_{2n+1}(t_{2n+1})\mathbf{G}_{2n+1}, \qquad (2)$$

where $\mathbf{M}_e$ denotes the homogeneous transformation matrix of the end-effector. Moreover, the rotations around the z-axis

$$\mathbf{M}_i(t_i) = \begin{pmatrix} 1 & 0 & 0 & 0 \\ 0 & \frac{1-t_i^2}{1+t_i^2} & -\frac{2t_i}{1+t_i^2} & 0 \\ 0 & \frac{2t_i}{1+t_i^2} & \frac{1-t_i^2}{1+t_i^2} & 0 \\ 0 & 0 & 0 & 1 \end{pmatrix},$$

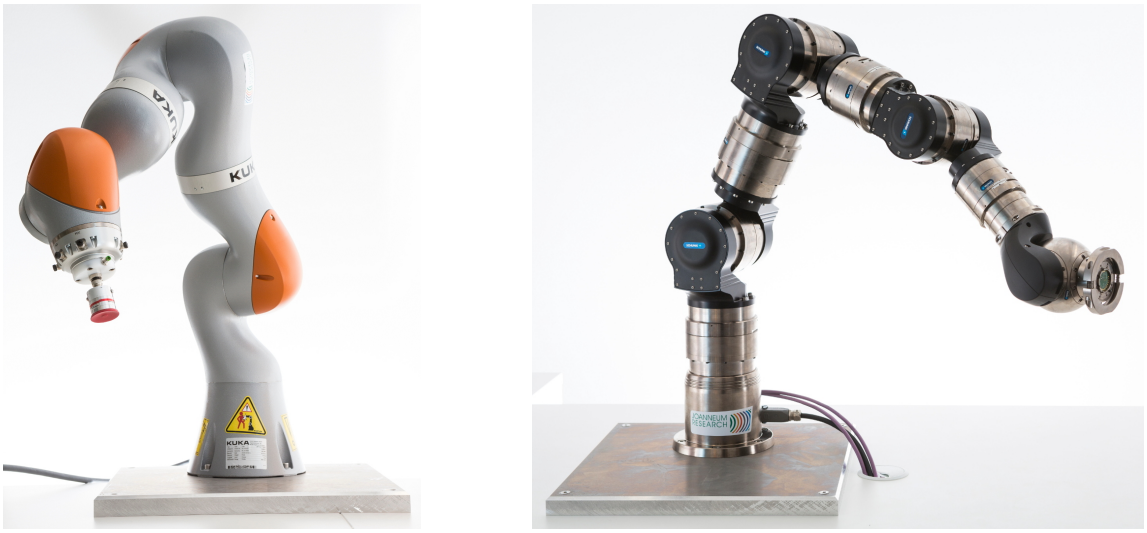

(a) KUKA LBR iiwa 7R. (b) Schunk LWA 9R.

Fig. 1: Two examples of redundant circular manipulators.

is used in Eq. (2) as well as the transformation matrices for the displacements

$$\mathbf{G}_i = \begin{pmatrix} 1 & 0 & 0 & 0 \\ a_i & 1 & 0 & 0 \\ 0 & 0 & \frac{1-w_i^2}{1+w_i^2} & -\frac{2w_i}{1+w_i^2} \\ d_i & 0 & \frac{2w_i}{1+w_i^2} & \frac{1-w_i^2}{1+w_i^2} \end{pmatrix},$$

where $t_i = \tan\left(\frac{\theta_i}{2}\right)$, $w_i = \tan\left(\frac{\alpha_i}{2}\right)$, θ_i, α_i, a_i, and d_i for $i = 1, 2, \ldots, 2n+1$ are given in Table I. Then we have the coordinate system for the manipulator with the origin at the shoulder P_s. Moreover, the z-axis is along the direction of the extension of the circular manipulators. Solving the inverse kinematics can now be reduced to the following procedure: Find all t_i for a given $\mathbf{M}_e$.

C. Dual Quaternion Notations

For the kinematic singularities computation, we choose the dual quaternions for the kinematic equations [23], [24], [25]. For describing SE(3), the group of maps from $\mathbb{R}^3$ to itself that preserve Euclidean distances and orientation, we employ $\mathbb{D} := \mathbb{R} + \epsilon\mathbb{R}$ the ring of dual numbers, with multiplication defined by $\epsilon^2 = 0$, and the quaternions $\mathbb{H}$, the non-commutative algebra, i.e., the $\mathbb{DH} := \mathbb{D} \otimes_{\mathbb{R}} \mathbb{H}$. The conjugation is taken from the quaternion conjugation. In addition, we have a $\mathbb{P}^7$ by projectivizing $\mathbb{DH}$ as a real 8-dimensional vector space. The Study condition [26] that $h\overline{h}$ is strictly real, i.e., its dual part is zero, is a homogeneous quadratic equation which is called the Study quadric, denoted by S. Let E be the linear 3-space representing all dual quaternions with zero primal part, which is contained in the Study quadric. The complement $S - E$ forms a Lie group, which is isomorphic to SE(3) (see [26, Sect. 2.4]).

Using Denavit-Hartenberg geometric invariant parameters [7], i.e., twist angles, orthogonal distances, and offsets, manipulators can determine the geometric structure of manipulators. Once the manipulator is assembled, we know all the rotation axes using the geometric invariants. Here, we use a nonzero dual quaternion h to represent a rotation (around with an axis) if and only if $h\overline{h}$ and $h + \overline{h}$ are strictly real and its primal vectorial part is nonzero. Furthermore, we take a new formulation of the forward kinematics in the language of dual quaternions for the kinematic singularities computation. The rotation with axis determined by $\mathbf{i}$ and angle q corresponds to the dual quaternion $(\cos(\frac{q}{2}) - \sin(\frac{q}{2})\mathbf{i})$, which is projectively equivalent to $(1 - \tan(\frac{q}{2})\mathbf{i})$. A formulation of the forward kinematics mapping is

$$(1 - t_1 h_1)(1 - t_2 h_2) \cdots (1 - t_n h_n) \equiv h_e, \tag{3}$$

where $h_1, \ldots, h_n$ are dual quaternions specifying the rotation axes in the initial position of the robot, the h_e is a dual quaternion specifying a pose of the end-effector, and the "$\equiv$" means projectively equivalent. The set G of all n-tuple $(t_1, \ldots, t_n) \in (\mathbb{P}^1)^n$ fulfilling Eq. (3) is called the *configuration set* (i.e., the inverse kinematics) of the robot arm with respect to a fixed pose h_e. In order to solve Eq. (3), one can multiply it with the conjugation $\overline{h_e}$ from both sides. Then a system of equations is obtained by comparing both sides as 8-dimensional vectors.

III. A Geometric Inverse Kinematics Solution for 7R Circular Manipulators

In this section, we first derive the closed-form solution symbolically. Using the closed-form solution, we give two numerical examples for demonstration.

A. Symbolic solutions computation

There are known closed-form solutions [1], [5], [8] for a 7R circular manipulator. We are going to show the symmetric inverse kinematics solution.

Let $P_w = [x, y, z]^T$ be the position of our end-effector, which we assume is the intersecting point of the last three axes

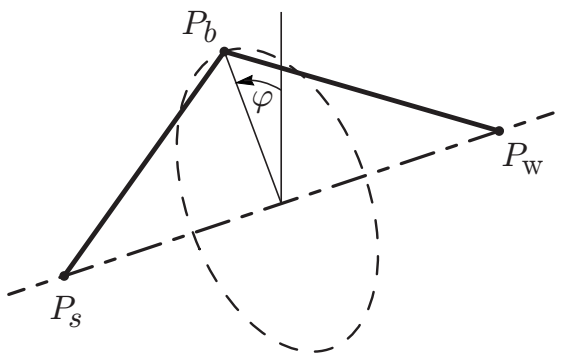

Fig. 2: The planar projection of the geometric structure of KUKA LBR iiwa 7R.

(the position of the wrist in the Cartesian coordinate system with the origin at the position of the elbow). The choice of the Denavit-Hartenberg parameters in the equation 2 gives a choice of the coordinate system. By the forward kinematics equation given in Eq. (2), we have

$$\mathbf{M}_e = \mathbf{M}_1(t_1)\mathbf{G}_1\mathbf{M}_2(t_2)\mathbf{G}_2\cdots\mathbf{M}_7(t_7)\mathbf{G}_7,$$

where

$$\mathbf{M}_e = \begin{pmatrix} 1 & \mathbf{0} \\ P_w & \mathbf{R} \end{pmatrix}.$$

First, we solve t_4 because it is always fixed when the 7R circular manipulators make the self-motion. There are two solutions [5], i.e.,

$$t_4^2 = \frac{(d_3+d_5)^2-x^2-y^2-z^2}{x^2+y^2+z^2-(d_3+d_5)^2}, \tag{4}$$

where d_3 and d_5 are offsets as given in Tab. I. The fourth joint (t_4) is always fixed if the end-effector is static. It is worth mentioning that the vanishing of the denominator of Eq. (4) gives the rotation 180 degrees which are out of the joint limit of the fourth joint.

Second, we follow the swivel angle notation defined by [8] which gives us a parameter to parametrize the closed-form solution for 7R circular manipulators. Let $P_b = [x_b, y_b, z_b]^T$ be the position of the elbow with a parameter $t = \tan(\varphi/2)$ (φ is the swivel angle in Fig. 2). We parameterize the P_b by the rotation around the axis, which goes through the shoulder P_s and the wrist P_w. Let M_e be a pose or a trajectory of the wrist. Then one can find a parametrization (swivel angle) of P_b by solving the elementary geometric problem as shown in Fig. 2. First, the radius of the circle in Fig. 2 is uniquely determined by the position of the wrist P_w. If the wrist's position is on the z-axis, i.e., we have $x^2 + y^2 = 0$, then, assuming that $z \neq 0$ (which is reasonable as the reach limit), the plane geometric constraint becomes simple. We assume that the wrist's position P_w is not always on the z-axis, i.e., we have $x^2 + y^2 \neq 0$. Then the point P_b^0 is found as the starting point for the parametrization (or the reference point for measuring the swivel angle φ), where

$$P_b^0 = [x_b^0, y_b^0, z_b^0]^T = \left[\frac{xuz+xv}{2w}, \frac{yuz+yv}{2w}, \frac{\left(x^2+y^2\right)u-v}{2w}\right]^T, \tag{5}$$

and $u = \sqrt{((d_3+d_5)^2-\nu^2)}\sqrt{(\nu^2-(d_3-d_5)^2)}$, $\nu^2 = x^2+y^2+z^2$, $v = \sqrt{\left(d_3^2-d_5^2+\nu^2\right)^2(x^2+y^2)}$, $w = \nu^2\sqrt{(x^2+y^2)}$, The parametrization of P_b is

$$P_b = [x_b, y_b, z_b]^T = \begin{bmatrix} \frac{((x^2-y^2-z^2)x_b^0+2x(yy_b^0+zz_b^0))t^2+(2y_b^0z-2yz_b^0)t+x_b^0}{1+(x^2+y^2+z^2)t^2} \\ \frac{((y^2-x^2-z^2)y_b^0+2y(xx_b^0+zz_b^0))t^2+(2xz_b^0-2x_b^0z)t+y_b^0}{1+(x^2+y^2+z^2)t^2} \\ \frac{((z^2-x^2-y^2)z_b^0+2z(xx_b^0+yy_b^0))t^2+(2x_b^0y-2xy_b^0)t+z_b^0}{1+(x^2+y^2+z^2)t^2} \end{bmatrix}, \tag{6}$$

where one needs to scale parameter t such that it corresponds to the tangent of the half of the swivel angle, i.e., a re-parametrization by replacing t with $\frac{t'}{\sqrt{x^2+y^2+z^2}}$ has to be done. In addition, by the forward kinematics of the first two rotation joints, we get

$$\begin{bmatrix} 1 \\ P_b \end{bmatrix} = \mathbf{M}_1\mathbf{G}_1\mathbf{M}_2\mathbf{G}_2 \begin{bmatrix} 1 \\ 0 \\ 0 \\ 0 \end{bmatrix} = \begin{bmatrix} 1 \\ -\frac{2d_3t_2(1-t_1^2)}{(1+t_1^2)(1+t_2^2)} \\ -\frac{4d_3t_1t_2}{(1+t_1^2)(1+t_2^2)} \\ \frac{d_3(1-t_2^2)}{(1+t_2^2)} \end{bmatrix}. \tag{7}$$

Therefore, two solutions for t_1, t_2 can be found:

$$t_1 = \frac{y_b}{x_b-\sqrt{d_3^2-z_b^2}}, \quad t_2 = \sqrt{\frac{d_3-z_b}{d_3+z_b}} \tag{8}$$

and

$$t_1 = \frac{y_b}{x_b+\sqrt{d_3^2-z_b^2}}, \quad t_2 = -\sqrt{\frac{d_3-z_b}{d_3+z_b}}, \tag{9}$$

where the vanishing of the denominator of Eq. (8) and Eq. (9) can happen at reach limit which is not a problem, or at $y_b = 0$ which gives us the simpler situation for the closed-form solutions that either t_1 or t_2 equals to zero (even both are zeros).

Third, we obtain the solution of t_3 using two pairs of solutions of t_1, t_2 and the position of the wrist $P_w = [x, y, z]$. By the forward kinematics of the first four rotation joints, we have

$$\begin{bmatrix} 1 \\ P_w \end{bmatrix} = \mathbf{M}_1\mathbf{G}_1\cdots\mathbf{M}_4\mathbf{G}_4 \begin{bmatrix} 1 \\ 0 \\ 0 \\ 0 \end{bmatrix} = \begin{bmatrix} 1 \\ x \\ y \\ z \end{bmatrix}, \tag{10}$$

where

$$\begin{aligned} x &= \tfrac{2d_3(t_1^2-1)t_2}{(1+t_1^2)(t_2^2+1)} - \tfrac{2d_5(1-t_1^2)t_2(1-t_4^2)}{(1+t_1^2)(1+t_2^2)(1+t_4^2)} + \\ &\quad \tfrac{8d_5t_1t_3t_4}{(1+t_1^2)(1+t_3^2)(1+t_4^2)} - \tfrac{2d_5(1-t_1^2)(1-t_2^2)(1-t_3^2)t_4}{(1+t_1^2)(1+t_2^2)(1+t_3^2)(1+t_4^2)}, \\ y &= -\tfrac{4d_3t_1t_2}{(1+t_2^2)(1+t_1^2)} - \tfrac{4d_5t_1t_2(1-t_4^2)}{(1+t_1^2)(1+t_2^2)(1+t_4^2)} - \\ &\quad \tfrac{4d_5(1-t_1^2)t_3t_4}{(1+t_1^2)(1+t_3^2)(1+t_4^2)} - \tfrac{4d_5t_1(1-t_2^2)(1-t_3^2)t_4}{(1+t_1^2)(1+t_2^2)(1+t_3^2)(1+t_4^2)}, \\ z &= \tfrac{d_3(1-t_2^2)}{1+t_2^2} + \tfrac{d_5(1-t_2^2)(1-t_4^2)}{(1+t_2^2)(1+t_4^2)} + \tfrac{4t_4t_2d_5(t_3^2-1)}{(1+t_2^2)(1+t_3^2)(1+t_4^2)}. \end{aligned} \tag{11}$$

This is an overdetermined system for solving t_3, which gives us a unique solution for t_3:

$$\begin{aligned} t_3 = &\tfrac{-2((d_3-d_5+z)t_4^2+d_3+d_5+z)t_1t_2^2-2y(t_4^2+1)(t_1^2+1)t_2}{((t_2^2+1)(t_4^2+1)z+(t_2^2-1)(t_4^2(d_3-d_5)+(d_3+d_5))-4d_5t_2t_4)(t_1^2-1)} \\ &- \tfrac{2((d_3-d_5-z)t_4^2+d_3+d_5-z)t_1}{((t_2^2+1)(t_4^2+1)z+(t_2^2-1)(t_4^2(d_3-d_5)+(d_3+d_5))-4d_5t_2t_4)(t_1^2-1)}. \end{aligned}$$

In case $t_1^2 = 1$, we need to pick the other formula

$$t_3 = \frac{((d_3-d_5+z)t_4^2+d_3+d_5+z)(t_1^2-1)t_2^2-2x(t_4^2+1)(t_1^2+1)t_2}{((t_2^2+1)(t_4^2+1)z+(t_2^2-1)(t_4^2(d_3-d_5)+(d_3+d_5))-4d_5t_2t_4)t_1} + \frac{((d_3-d_5-z)t_4^2+d_3+d_5-z)(t_1^2-1)}{((t_2^2+1)(t_4^2+1)z+(t_2^2-1)(t_4^2(d_3-d_5)+(d_3+d_5))-4d_5t_2t_4)t_1}.$$

Notice that the denominator can still vanish, defining the rotation range for the swivel angle ϕ.

Fourth, we can solve t_5, t_6, t_7 as in [5], [26] using the information we obtained for t_1, t_2, t_3. Here we want to say more words. We can solve t_5, t_6, t_7 without using t_1, t_2, t_3 by symmetry which is similar to how we solved t_1, t_2, t_3.

Let $P_s' = [x', y', z']$ be the position of the shoulder in the coordinate system with its origin at the wrist point W. It can be obtained by the inverse of $\mathbf{M}_e$:

$$\begin{bmatrix} 1 \\ P_s' \end{bmatrix} = \mathbf{M}_e^{-1} \begin{bmatrix} 1 \\ 0 \\ 0 \\ 0 \end{bmatrix} = \begin{bmatrix} 1 \\ x' \\ y' \\ z' \end{bmatrix}$$

Similarly, by Eq. (10) we can obtain the closed-formula for x', y', z' with t_7, t_6, t_5, t_4:

$$x' = -\frac{(2d_5t_6(t_7^2-1)}{(1+t_6^2)(1+t_7^2)} - \frac{2d_3(1-t_4^2)t_6(1-t_7^2)}{(1+t_4^2)(1+t_6^2)(1+t_7^2)} + \frac{8d_3t_4t_5t_7}{(1+t_4^2)(1+t_5^2)(1+t_7^2)} - \frac{2d_3t_4(1-t_5^2)(1-t_6^2)(1-t_7^2)}{(1+t_4^2)(1+t_5^2)(1+t_6^2)(1+t_7^2)},$$

$$y' = \frac{4d_5t_6t_7}{(1+t_6^2)(1+t_7^2)} + \frac{4d_3t_7t_6(1-t_4^2)}{(1+t_4^2)(1+t_6^2)(1+t_7^2)} + \frac{4d_3t_4t_5(1-t_7^2)}{(1+t_4^2)(1+t_5^2)(1+t_7^2)} + \frac{4d_3t_4(1-t_5^2)(1-t_6^2)t_7}{(1+t_4^2)(1+t_5^2)(1+t_6^2)(1+t_7^2)},$$

$$z' = \frac{d_5(t_6^2-1)}{(1+t_6^2)} + \frac{d_3(1-t_6^2)(t_4^2-1)}{(1+t_4^2)(1+t_6^2)} + \frac{4d_3t_4t_6(1-t_5^2)}{(1+t_4^2)(1+t_5^2)(1+t_6^2)}.$$

Let $P_b' = [x_b', y_b', z_b']^T$ be the position of the elbow in the coordinate system with the origin at the wrist again. This is obtained similar as P_b with considering the reverse serial manipulator, namely, one needs to exchange d_3 and d_5 in Eq. (5) and Eq. (6). In the second, one needs to replace x, y, z by x', y', z' in Eq. (5) and Eq. (6) as well. In addition, we can find the symbolic position of the elbow in the Cartesian coordinate system with the origin at the intersecting point of the last three axes (wrist). We get

$$P_b' = \left[\frac{2d_5t_6(t_7^2-1)}{(1+t_7^2)(1+t_6^2)}, \frac{4d_5t_7t_6}{(1+t_7^2)(1+t_6^2)}, \frac{d_5(t_6^2-1)}{(1+t_6^2)}\right]$$

by the forward kinematics of the last two rotation joints (reverse rotation makes the formula different to Eq. (7)). Therefore, we get two solution for t_6, t_7:

$$t_7 = \frac{y_b'}{\sqrt{d_5^2-{z_b'}^2}-x_b'}, \quad t_6 = \sqrt{\frac{d_5+z_b'}{d_5-z_b'}}, \qquad or$$

$$t_7 = -\frac{y_b'}{x_b'+\sqrt{d_5^2-{z_b'}^2}}, \quad t_6 = -\sqrt{\frac{d_5+z_b'}{d_5-z_b'}},$$

where the situation for the vanishing of the denominators is similar to the t_1 or t_2. Then the position of the shoulder $P_s = [x', y', z']$ (in the Cartesian coordinate system with origin at W) is computed by taking the inverse of M_e. By the overdetermined system regarding x', y', z', we can find a unique solution for t_5:

$$t_5 = \frac{-2((d_3-d_5+z')t_4^2-d_3-d_5+z)t_7t_6^2-2y'(t_4^2+1)(t_7^2+1)t_6}{((t_6^2+1)(t_4^2+1)z+(t_6^2-1)(t_4^2(d_3-d_5)-(d_3+d_5))+4d_3t_6t_4)(t_7^2-1)} - \frac{2((d_3-d_5-z')t_4^2-d_3-d_5-z')t_7}{((t_6^2+1)(t_4^2+1)z+(t_6^2-1)(t_4^2(d_3-d_5)-(d_3+d_5))+4d_3t_6t_4)(t_7^2-1)}$$

or

$$t_5 = \frac{(t_7^2-1)((d_3-d_5+z')t_4^2-d_3-d_5+z')t_6^2}{2((t_6^2+1)(t_4^2+1)z+(t_6^2-1)(t_4^2(d_3-d_5)-(d_3+d_5))+4d_3t_6t_4)t_7} + \frac{2x'(t_7^2+1)(t_4^2+1)t_6+((d_3-d_5-z')t_4^2-d_3-d_5-z')(t_7^2-1)}{2((t_6^2+1)(t_4^2+1)z+(t_6^2-1)(t_4^2(d_3-d_5)-(d_3+d_5))+4d_3t_6t_4)t_7},$$

where the situation for the vanishing of the denominators is similar to the t_3.

In general, for each swivel angle (a specific position of the elbow), we have eight solutions. Furthermore, if we know one of these eight solutions, the other seven can be obtained by a symmetric change of angles. Let t_1, t_2, t_3, t_4, t_5, t_6, t_7 be a solution, then the eight solutions are

$$\left\{\begin{array}{ccccccc} t_1, & t_2, & t_3, & t_4, & t_5, & t_6, & t_7 \\ -\frac{1}{t_1}, & -t_2, & -\frac{1}{t_3}, & t_4, & t_5, & t_6, & t_7 \\ t_1, & t_2, & t_3, & t_4, & -\frac{1}{t_5}, & -t_6, & -\frac{1}{t_7} \\ -\frac{1}{t_1}, & -t_2, & -\frac{1}{t_3}, & t_4, & -\frac{1}{t_5}, & -t_6, & -\frac{1}{t_7} \\ t_1, & t_2, & -\frac{1}{t_3}, & -t_4, & -\frac{1}{t_5}, & t_6, & t_7 \\ -\frac{1}{t_1}, & -t_2, & t_3, & -t_4, & -\frac{1}{t_5}, & t_6, & t_7 \\ t_1, & t_2, & -\frac{1}{t_3}, & -t_4, & t_5, & -t_6, & -\frac{1}{t_7} \\ -\frac{1}{t_1}, & -t_2, & t_3, & -t_4, & t_5, & -t_6, & -\frac{1}{t_7} \end{array}\right\}.$$

If a t_i is zero (for $i = 1, \ldots, 7$), then $\pm\frac{1}{t_i}$ corresponds to a rotation of 180 degree.

B. Numerical examples

The first example presented in this paper is about the inverse kinematics solution of a 7 DoF circular manipulator with a given pose. We take the KUKA LBR iiwa 14 as our candidate for this demonstration. In this case $d_3 = 21/50$ and $d_5 = 2/5$ with unit in m (meter). Let

$$t_1 = \tfrac{5}{4}, t_2 = \tfrac{3}{5}, t_3 = -\tfrac{3}{11}, t_4 = -\tfrac{1}{8}, t_5 = -\tfrac{1}{9}, t_6 = \tfrac{1}{9}, t_7 = \tfrac{8}{7}$$

be a starting posture with the pose $\mathbf{M}_e$ as:

$$\begin{pmatrix} 1 & 0 & 0 & 0 \\ \frac{444999}{2265250} & -\frac{37249225411}{43029103325} & -\frac{20358343848}{43029103325} & \frac{732768}{4479865} \\ -\frac{9502492}{14724125} & \frac{71934541176}{559378343225} & -\frac{294204751257}{559378343225} & -\frac{48963088}{58238245} \\ \frac{32924}{71825} & \frac{264030432}{545734969} & -\frac{385709744}{545734969} & \frac{146631}{284089} \end{pmatrix}$$

In Fig. 3, we show the variation of the inverse kinematics solution with swivel angle parameter ϕ (the range from approximate -100 degrees to 60 degrees) for a fixed pose as above. The left figure shows a variation of the joint angles (q_i, where $t_i = \tan(q_i/2)$, and the range from approximate -180 degrees to 180 degrees) and the right figure shows a variation of the cost function $g = \sum q_i^2$. Global information on the variation of the joint angles gives the possibility for further optimization. One can see that the cost function has a global minimal (notice that this is in one of the eight solutions) among the interval of the swivel angles. The global minimal can be found using the closed-form solution, and a controlling strategy of the swivel angle can be applied. For further optimization procedures, we leave it for future study. A strategy for choosing an optimal swivel angle can be based on obstacle avoidance. The inverse kinematics near a kinematic singularity is shown in Fig. 8.

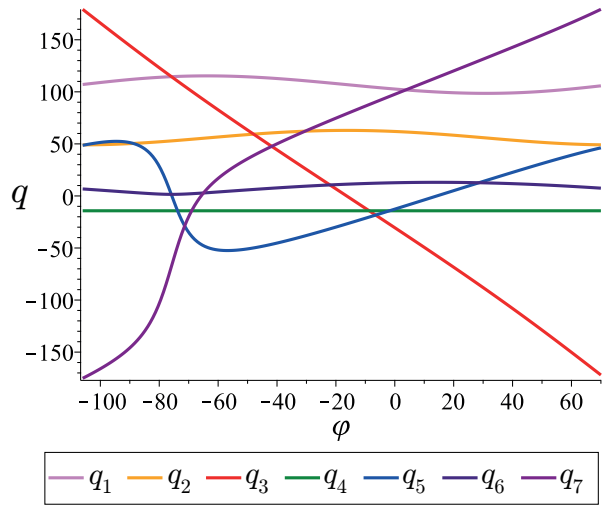

(a) The individual q_i variation.

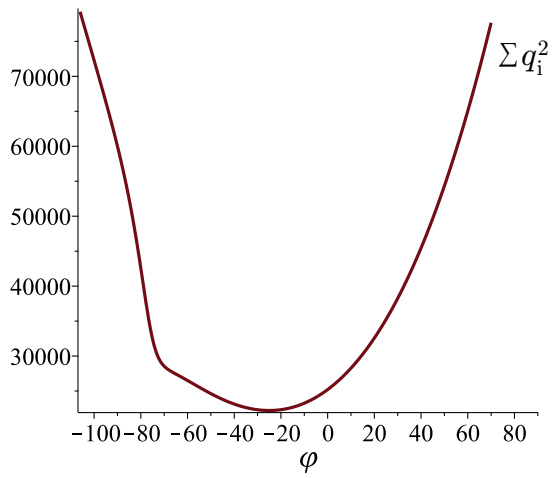

(b) The summation variation.

Fig. 3: The self-motion in terms of q_i and the cost function variation along the feasible interval of the swivel angle ϕ.

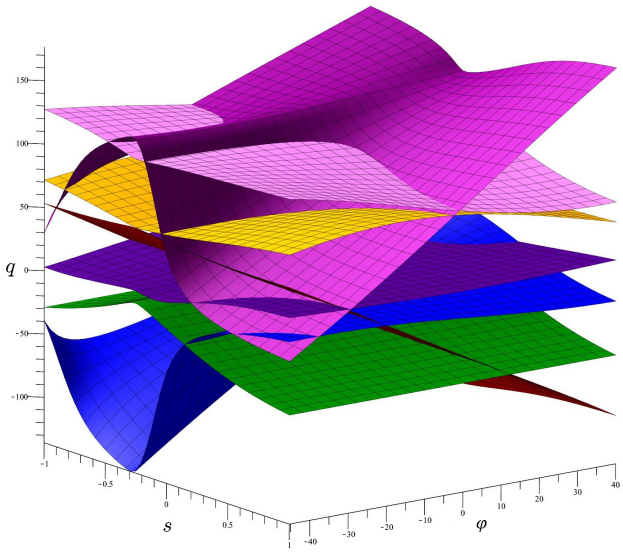

(a) The individual q_i variation.

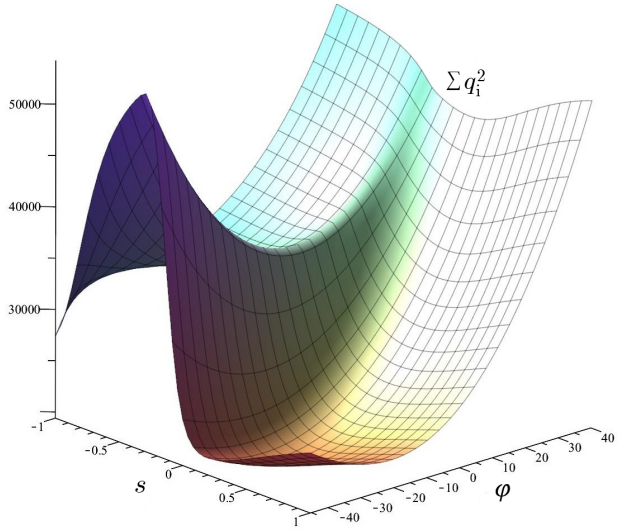

(b) The summation variation.

Fig. 4: The actual possible self-motion of q_i and the variation of the cost function alongs with the parameters ϕ and s.

The second example treats with the same manipulator structure as before, with the same starting posture (the pose is $\mathbf{M}_e$), and a given trajectory of the end-effector as:

$$\mathbf{M}_e(s) = \mathbf{M}_e + \begin{pmatrix} 1 & 0 & 0 & 0 \\ -\frac{s}{5(s^2+1)} & 0 & 0 & 0 \\ 0 & 0 & 0 & 0 \\ -\frac{s^2}{5(s^2+1)} & 0 & 0 & 0 \end{pmatrix}$$

where s is the parameter of the trajectory. By substituting all values to the closed-form solution in Section III-A, one can obtain the parametrization of each q_i with the parameters ϕ and s. These formulas are too long to present all here. Nevertheless, we will show the variation of these functions on the parameters ϕ and s. Therefore, in Fig. 4 we show the variation of the inverse kinematics solution with the swivel angle parameter ϕ for a pose trajectory parametrized by s as given above. The left figure shows a variation of the rotation angles (q_i), and the right figure shows a variation of the cost function $g = \sum q_i^2$. These two figures show an overview of the redundancy variation along the wrist trajectory $P_w(s)$. Global information on the variation of the joint angles regarding the fixed trajectory gives a rich optimization possibility. The cost function regarding the joint limit has a local minimum for each instance s. The global minimum regarding an interval of the trajectory needs a more detailed optimization procedure. Especially when there are singularities in the inverse kinematic solution, the question arises of whether the global minimum can happen at a kinematic singularity? It is still an open issue for the authors too. The core focus of the paper is to give the closed-form inverse kinematics and the singularities analysis;

we leave the detailed optimization procedures for future study.

IV. Redundancy analysis for circular manipulators

Without loss of generality, we can assume that integer $n \geq 3$. For $n = 0, 1, 2$, the inverse kinematics problem leads to solving a trivial spherical geometric problem; whenever $n \geq 3$, a ($2n$+1)R circular manipulator is always kinematically redundant, and there is a $2n$-5 dimensional solution set for the inverse kinematics with a six DOF task. One can follow the automatic procedure for solving inverse kinematics solution from [21], namely, one can choose a parametrization for this solution set by assuming some rotational angles as parameters, e.g., we can choose the first (not necessary) $t_1, \ldots, t_{2n-5}$ as the free variables [2], [27] for solving the inverse kinematics. With the specialization of the ($2n$+1)R circular manipulator, we can decompose the ($2n$+1)R to a combination of 7R and ($2n$-6)R, where the closed-form 7R is known, and the ($2n$-6)R part is independent. It enables us to choose independent joint angles and gives us flexibility for picking closed-form solutions for ($2n$+1)R circular manipulators. The critical criteria for choosing the combination is that one needs to keep the properties of the 7R part, which needs to be the circular manipulators.

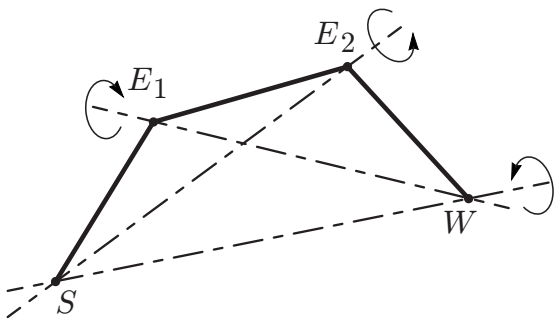

Fig. 5: The planar projection of the geometric structure of the Schunk 9R manipulator.

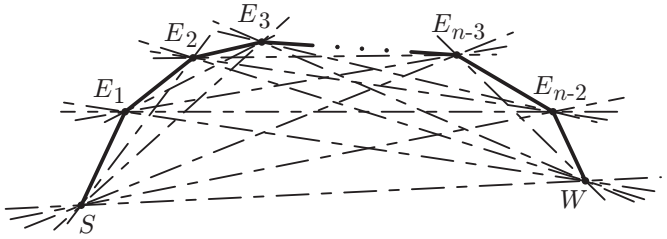

Fig. 6: The planar projection of the geometric structure of the ($2n$+1)R manipulator.

A. The 9R circular manipulators

If $n = 4$, then we deal with a 9R circular manipulator. One example of this structure is the Schunk LWA 4D 9 DoF, as shown in Fig. 1. From the schematic representation of this manipulator (see Fig. 5), one can observe that the last 7R or first 7R equals the previously discussed 7R circular manipulator. Using this knowledge, one will find two choices to solve the inverse kinematics problem of a 9R circular manipulator with closed-form. By the forward kinematics Eq. (2), we have

$$\mathbf{M}_e = \mathbf{M}_1(t_1)\mathbf{G}_1\mathbf{M}_2(t_2)\cdots\mathbf{M}_9(t_9)\mathbf{G}_9.$$

For the two choices of different 7R circular manipulators the deformed forward kinematics equation are:

$$\begin{aligned}\mathbf{M}_e^I &= \mathbf{M}_e\mathbf{G}_9^{-1}\mathbf{M}_9^{-1}(t_9)\mathbf{G}_8^{-1}\mathbf{M}_8^{-1}(t_8)\\ &= \mathbf{M}_1(t_1)\mathbf{G}_1\mathbf{M}_2(t_2)\cdots\mathbf{M}_7(t_7)\mathbf{G}_7,\end{aligned}$$

and

$$\begin{aligned}\mathbf{M}_e^{II} &= \mathbf{G}_2^{-1}\mathbf{M}_2^{-1}(t_2)\mathbf{G}_1^{-1}\mathbf{M}_1^{-1}(t_1)\mathbf{M}_e\\ &= \mathbf{M}_3(t_3)\mathbf{G}_3\mathbf{M}_4(t_4)\mathbf{G}_4\cdots\mathbf{M}_9(t_9)\mathbf{G}_9.\end{aligned}$$

By substituting with new x, y, z (comes from either $\mathbf{M}_e^I$ or $\mathbf{M}_e^{II}$) and offsets d_3, d_5 (or shifted subscripts by 2 from d_5, d_7) to the closed-form solution we derived in Section III-A, we can parametrize the rotation parameters $t_1, t_2, \ldots, t_9$ either by $\{t, t_1, t_2\}$ or $\{t, t_9, t_8\}$, where t is the swivel parameter.

In Fig. 5, there is another axis (the dashed line passing through S and W) which can be treated as another self-rotation motion. One can solve this self-rotation motion by fixing the three middle joints (joint $4, 5, 6$) of the 9R chain and only considering the first three R-joints and the last three R-joints. As we know that the Hooke linkage [24] is a combination of such two spherical joints (e.g., shoulder, wrist), in this case, one can use the closed-form solution from the Hooke linkage, which is a closed 6R linkage, e.g., closure equations from [28]. In addition, it can be obtained approximately by combining the motion produced by the other two axes (the dashed lines $\overline{SE_2}$ and $\overline{E_1W}$). Namely, solving an optimization problem minimizes the difference in the fixed rotation angles of the t_4, t_5, t_6.

B. Geometric representations of closed-form solutions

The swivel angle described in [8] is used to parametrize the one DOF inverse kinematics solution. This swivel angle corresponds to a rotation around an axis that goes through the center points (the shoulder and the twist points). In this case, one can have similar geometric arguments for ($2n$+1)R circular manipulators. The schematic expression of the general structure is shown in Fig. 6. There are rotations for the representation of the inverse kinematics solutions. How many rotations are there? The same number can be asked for the rotational axes. In total, there are $(n-1)(n-2)/2$ rotational axes (circles). A ($2n$+1)R circular manipulator has a $2n$-5 dimensional solution set for the inverse kinematics but on the other hands one can find $(n-1)(n-2)/2$ different rotation axes, which would cause $(n-1)(n-2)/2$ different "one-dimensional" solution sets for the inverse kinematics. Each "one-dimensional" solution is obtained from the $2n$-5 dimensional solution set by fixing $2n$-6 rotation joints.

We derive the formula of the number of axes by counting the connection of the center points of ($2n$+1)R circular manipulators. Note that there are n center points. The connection of two points gives us one line (axis) to determine a circle (rotation). There are $n(n-1)/2$ connections in total but not

all connections give us circles. There are adjacent connections that do not lead to valid rotations. In total, there are $n-1$ such connections. For this reason, the number of useful connections n_c can be defined to be $n_c = \frac{n(n-1)}{2} - (n-1) = \frac{(n-1)(n-2)}{2}$.

V. Kinematic singularities

A. Computation setting

Kinematic singularities are denoted as an algebraic variety (see [29] and the references there) defined by the 6×6 minors of the Jacobian matrix of the forward kinematics. In addition, we know that (see [30]) the Jacobian matrix is singular only if all rotation axes are contained in a linear line complex. With our kinematic setting, the oriented lines are set as purely vectorial dual quaternions with norm 1. We denote those lines by h_i for $s = 1, \dots, n$, corresponding to the i-th rotation axis in some initial configuration, where $h_i^2 = -1$ and denote the tangent of the half of the i-th rotation angle by t_i. In the coordinate frame of a middle link (the j-th and $j+1$-th axes) of the serial manipulator, the corresponding position of each oriented line can be easily computed as:

$$
\begin{aligned}
H_1 &= (1+t_j h_j)\cdots(1+t_2h_2)h_1(1-t_2h_2)\cdots(1-t_jh_j),\\
&\vdots\\
H_{j-1} &= (1+t_jh_j)h_{j-1}(1-t_jh_j),\\
H_j &= h_j,\\
H_{j+1} &= h_{j+1},\\
H_{j+2} &= (1-t_{j+1}h_{j+1})h_{j+2}(1+t_{j+1}h_{j+1}),\\
&\vdots\\
H_n &= (1+t_{j+1}h_{j+1})\cdots(1+t_{n-1}h_{n-1})h_n\\
&\quad (1-t_{n-1}h_{n-1})\cdots(1+t_{j+1}h_{j+1}).
\end{aligned}
$$

For instance, we have

$$
\begin{aligned}
H_1 &= (1+t_3h_3)(1+t_2h_2)h_1(1-t_2h_2)(1-t_3h_3),\\
H_2 &= (1+t_3h_3)h_2(1-t_3h_3),\\
H_3 &= h_3,\\
H_4 &= h_4,\\
H_5 &= (1+t_4h_4)h_5(1-t_4h_4),\\
H_6 &= (1+t_4h_4)(1+t_5h_5)h_6(1-t_5h_5)(1-t_4h_4),\\
H_7 &= (1+t_4h_4)(1+t_5h_5)(1+t_6h_6)h_7(1-t_6h_6)\\
&\quad (1-t_5h_5)(1-t_4h_4).
\end{aligned}
$$

The necessary conditions for these lines lie in a linear line complex. These are the determinants of all 6×6 minors of the Jacobian matrix whose columns are the coefficients of $H_1, \dots, H_n$ (see [30]). Each column has six entries from the Plücker coordinates of H_i, namely, the vectorial part of dual quaternion H_i. By the assumption of $h_i^2 = -1$, the scalar parts of dual quaternions H_i are zeroes.

B. Examples

The KUKA iiwa is a comprehensive example for our kinematic singularity analysis. We take the KUKA iiwa's home position as depicted in Fig. 7 with Denavit-Hartenberg parameters in Table II.

Fig. 7: KUKA LBR iiwa 7R.

TABLE II: Denavit-Hartenberg geometric parameter assignment of KUKA LBR iiwa 7R.

i-th Link	a_i	d_i (mm)	α_i	θ_i
1	0	d_1	90	θ_1
2	0	0	-90	θ_2
3	0	d_3	90	θ_3
4	0	0	-90	θ_4
5	0	d_5	90	θ_5
6	0	0	-90	θ_6
7	0	d_7	0	θ_7

A home position can be taken as:

$$
h_1 = \mathbf{k}, \quad h_2 = \mathbf{i}, \quad h_3 = \mathbf{k},\\
h_4 = \mathbf{i} - d_3\epsilon\mathbf{j}, \quad h_5 = \mathbf{k}, \quad h_6 = \mathbf{i} - (d_3+d_5)\epsilon\mathbf{j}, \quad h_7 = \mathbf{k}.
$$

By the definition of the Jacobian matrix using dual quaternions, the variety of kinematic singularities is defined by $\binom{7}{6} = 7$ polynomials (minors):

$$
\begin{aligned}
I = \langle & 8d_5(t_5-1)(t_5+1)t_4^2d_3^2t_2(t_3^2+1)^2,\\
& -32d_5t_4^2t_5t_6d_3^2t_2(t_3^2+1)^2, -8d_5t_4d_3t_2(t_3^2+1)^2(t_5^2+1)\\
& (d_3t_4^2t_5^2t_6 - d_3t_4t_5^2t_6^2 - d_5t_4^2t_5^2t_6 + d_3t_4^2t_6 + d_3t_4t_5^2 +\\
& d_3t_4t_6^2 - d_3t_5^2t_6 - d_5t_4^2t_6 - d_5t_5^2t_6 - d_3t_4 - d_3t_6 - d_5t_6),\\
& -8d_3d_5^2t_4^2t_6(t_5^2+1)^2(t_4^2+1)(t_3-1)(t_3+1),\\
& 32d_5^2t_4^2d_3t_2t_3t_6(t_5^2+1)^2(t_4^2+1), 0,\\
& -8d_5t_4d_3t_6(t_5^2+1)^2(t_4^2+1)(t_3^2+1)(d_3t_2t_3^2t_4^2 -\\
& d_5t_2^2t_3^2t_4 - d_5t_2t_3^2t_4^2 + d_3t_2t_3^2 + d_3t_2t_4^2 + d_5t_2^2t_4\\
& + d_5t_2t_3^2 - d_5t_2t_4^2 + d_5t_3^2t_4 + d_3t_2 + d_5t_2 - d_5t_4)\rangle.
\end{aligned}
$$

As we are interested in the real configurations, the quadratic factors t_i^2+1 and the geometric parameters d_3, d_5 do not vanish. The ideal I can be simplified by factoring out those quadratic factors. Then we have

$$
I' = \langle t_6t_2t_4^2, t_2t_4^2(t_5-1)(t_5+1), t_4^2t_6(t_3-1)(t_3+1)\rangle.
$$

It would be useful to keep the non-radical information for further study of each singularity in more detail. For the core of this paper, it is enough only to consider the radical ideal

because we are interested in the configurations which give the kinematic singularities. Then its radical ideal (see [31]) is

$$I_3 = \langle t_2 t_4 t_6, t_2 t_4 (t_5^2 - 1), t_4 t_6 (t_3^2 - 1) \rangle. \tag{12}$$

The prime decomposition of this ideal gives us six components:

$$\langle t_4 \rangle, \langle t_2, t_6 \rangle, \langle t_2, t_3 - 1 \rangle, \langle t_2, t_3 + 1 \rangle, \langle t_6, t_5 - 1 \rangle, \langle t_6, t_5 + 1 \rangle.$$

Remark 1: As the manipulator has the joint limit at the rotation of 180 degrees, we take $(1 - t_i h_i)$ for parameterizing the rotation of the i-th axis instead of using the homogeneous coordinates $(s_i - t_i h_i)$ to compute the singularities. In other words, the real (or physical reachable) singularities are computed by using $(1 - t_i h_i)$.

At singular configurations, the inverse kinematics or the configuration set becomes interesting, especially the singularity when the third angle in a 3R spherical set is 90 degrees (e.g., $t_3 = 1$). We take the KUKA LBR iiwa 14 for our numerical analysis of this special phenomenon, where $d_3 = 21/50, d_5 = 2/5$:

Singular configurations $t_2 = 0$ or $t_6 = 0$: Take a pose that can be reached by a singular posture

$$t_1 = \frac{3}{4}, t_2 = 0, t_3 = -1, t_4 = \frac{1}{2}, t_5 = -\frac{1}{4}, t_6 = 1, t_7 = -\frac{1}{4}.$$

The case for $t_6 = 0$ is similar. By the forward kinematics, the pose is

$$\frac{256}{192} - \mathbf{i}\left(-\frac{185}{384} - \frac{273}{1280}\epsilon\right) + \mathbf{j}\left(\frac{65}{28} + \frac{259}{1280}\epsilon\right) + \mathbf{k}\frac{15}{64}.$$

Using Gröbner Basis [24] for the closed loop of linkages (fixing the end-effector gives us a closed loop), we can find all other configurations for the pose. By a symbolic method, we have a constraint ideal (whose polynomials are too much to show here) for all configurations:

$$\begin{aligned} I_c = &\langle 4t_4^2 - 1, 825t_1^2t_2^2 + 384t_1^2t_2 + 224t_1t_2 + 825t_2^2 \\ &- 384t_2, -825t_1t_2^2 + 112t_1t_2t_3 - 800t_1t_2t4 + \\ &825t_2^2t_3 - 384t_2t_3, 825t_1t_2 - 56t_1t_3 + 400t_1t_4 \\ &- 825t_2t_3 + 400t_3t_4 + 192t_1 + 192t_3 + 56, \ldots \rangle. \end{aligned} \tag{13}$$

With the prime decomposition of the ideal I_c in Eq. (13), the configuration set has six components (all are 1-dimensional components):

$$\begin{aligned} &\langle 2t_4 - 1, t_2, -4 + t_7, t_5 - 4, t_6 + 1, t_1t_3 - 7t_1 - 7t_3 - 1 \rangle, \\ &\langle 2t_4 + 1, t_2, -4 + t_7, t_5 - 4, t_6 + 1, 7t_1t_3 + t_1 + t_3 - 7 \rangle, \\ &\langle 2t_4 - 1, t_2, 1 + 4t_7, 4t_5 + 1, t_6 - 1, t_1t_3 - 7t_1 - 7t_3 - 1 \rangle, \\ &\langle 2t_4 + 1, t_2, 1 + 4t_7, 4t_5 + 1, t_6 - 1, 7t_1t_3 + t_1 + t_3 - 7 \rangle, \\ &\langle 2t_4 - 1, t_1t_3 + 7t_1 - 7t_3 + 1, 825t_2t_3 - 825t_1t_2 \ldots \rangle, \\ &\langle 2t_4 + 1, 7t_1t_3 - t_1 + t_3 + 7, 825t_2t_3 - 825t_1t_2 \ldots \rangle. \end{aligned} \tag{14}$$

We can find that all singularities happen at the intersection of the components as in Fig. 8. When we fix the end-effector, the obstacle avoidance is done by switching the swivel angle. However, the first four motion components (where the polynomial t_2 appears in the first four ideals of Eq. (14)) do not affect the obstacles avoidance when we fix the end-effector because the elbow point position is not changing during such four motion modes. In Fig. 8, the red curves are such modes. Suppose the robot instantaneously is in such a mode for completing the obstacle avoidance for the elbow point. In that case, we have to let the manipulator pass through the kinematic singularities (the intersection) and switch to the other components (last two of Eq. (14) which are either the green curves or the blue curves in Fig. 8). In other words, we control the robot along a red curve and switch to a green/blue curve by passing through the intersection. In Fig. 8, it is worth noticing that some curves are not connected because it is reaching the joint limit (180 degrees). Notice that this inverse kinematics analysis can also be achieved using the closed-form solution in Section III. As the self-motion has the singularity at $t_2 = 0$, Eq. 8 and Eq. 9 are not enough for solving t_1 and t_3. Using the Eq. 11, there is a motion mode that the t_1 and the t_3 are compensated each other, i.e., the red curve in Fig. 8. Moreover, the bifurcation points in Fig. 8 correspond to the places of the zero swivel angle.

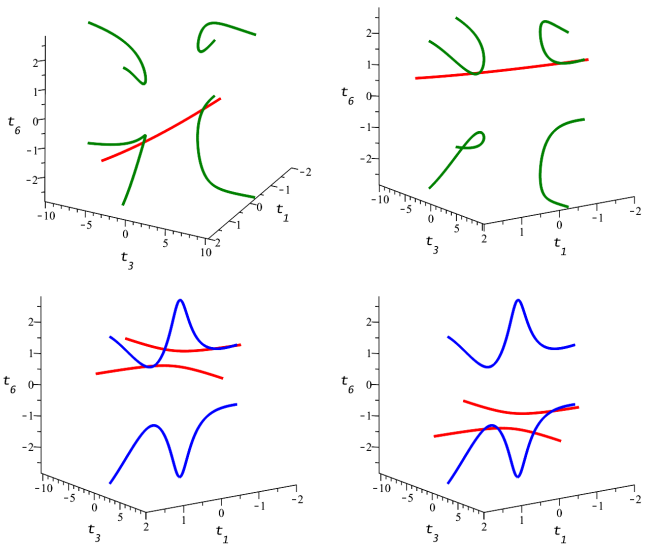

Fig. 8: The projection of partial solutions onto the $t_1t_3t_6$-space

Remark 2: We can pass through the kinematic singularities in our situation because we have enough motors to control the manipulators. The critical points (bifurcation singularities) are the points where $t_2 = 0$ and $t_3 = \pm 1$.

C. Recursive Generating Singular Loci

By a brute force method, and with the initial position (home position) as:

$$\begin{aligned} &h_1 = \mathbf{k}, \quad h_2 = \mathbf{i}, h_3 = \mathbf{k}, \\ &h_4 = \mathbf{i} - d_3\epsilon\mathbf{j}, \quad h_5 = \mathbf{k}, \quad h_6 = \mathbf{i} - (d_3 + d_5)\epsilon\mathbf{j}, \\ &h_7 = \mathbf{k}, h_8 = \mathbf{i} - (d_3 + d_5 + d_7)\epsilon\mathbf{j}, \quad h_9 = \mathbf{k}, \end{aligned}$$

we obtain the variety of kinematic singularities, which is generated by $\binom{9}{6} = 84$ polynomials (minors). As we are only interested in real configurations and the geometric parameters

d_3, d_5 do not vanish, we have a radical ideal, by factoring out the quadratic factors t_i^2+1,

$$\begin{aligned} I_4 = \langle & t_2t_4(t_5^2-1), t_2t_4t_6, (t_3^2-1)t_4t_6 \\ & t_2t_4t_7, t_2t_4t_8, (t_3^2-1)t_4t_7, (t_3^2-1)t_4t_8, \\ & t_2t_6(t_7^2-1), t_3t_6(t_7^2-1), t_2t_6t_8, t_3t_6t_8, \\ & t_4t_6(t_7^2-1), t_4t_6t_8, (t_5^2-1)t_6t_8 \rangle. \end{aligned} \tag{15}$$

If $n=4$, then we deal with a 9R circular manipulator. One example of this structure is the Schunk LWA 4D 9 DoF, as shown in Fig. 1. From the schematic representation of this manipulator (see Fig. 5), one can observe that the last 7R or first 7R equals the previously discussed 7R circular manipulator. By comparing the Eq. (12) and the Eq. (15), we found three patterns such that $I_4 = I_3 + K_3 + I_3'$:

- $I_3 \subset I_4$
- $I_3' \subset I_4$
- $K_3 \subset I_4$.

where I_3' is obtained by replacing each t_i by t_{i+2} as

$$I_3' = \langle t_4t_6(t_7^2-1), t_4t_6t_8, (t_5^2-1)t_6t_8 \rangle,$$

K_3 is obtained by two parts

$$t_2t_4t_7, t_2t_4t_8, (t_3^2-1)t_4t_7, (t_3^2-1)t_4t_8$$

and

$$t_3t_6t_8, t_2t_6t_8, t_3t_6(t_7^2-1), t_2t_6(t_7^2-1)$$

One can see that they are symmetric by reversing the order of indices $2, \ldots, 8$. The first part is obtained by modifying some polynomials of I_3 by replacing the last index entry (e.g., t_6) with further two entries (e.g., t_7, t_8), which we call the index extension. The second part is obtained by replacing each t_i by t_{10-i} from the first part. We have the generic formula:

$$I_{n+1} = \langle I_n, K_n, I_n' \rangle.$$

We have checked the above conjecture for $n = 5, 6, 7$ with a brute force method which confirms (see Appendix. A). Recall that the prime decomposition of I_3 has six components (all are linear subspaces, i.e., hyperplanes or intersection of hyperplanes, and we ignore other eight linear subspaces where t_2, t_4, t_6 could be infinity corresponding to the rotations of 180 degrees):

$$\langle t_4 \rangle, \langle t_2, t_6 \rangle, \langle t_2, t_3 \pm 1 \rangle, \langle t_6, t_5 \pm 1 \rangle.$$

The prime decompositions of I_4, I_5, I_6, I_7 are the intersections of $15, 28, 45, 66$ planes, respectively. One can conjecture that the singularities for a $2n+1$ circular manipulator are the intersection of $(n-1)(2n-3)$ hyperplanes. Notice that we ignore the rotations of 180 degrees.

VI. Discussion of Results and Future Research

This paper deals with the kinematic analysis of serial manipulators with a particular structure introduced as circular manipulators. We first recalled the closed-form solution of circular manipulators when n=3 and showed the pattern of closed-form solutions. The novel idea of this solution is that we give the explicit expressions for each joint based on the self-motion parameter (swivel angle). It solves all angles simultaneously, which differs from others, which solve the first three joint angles first and the other three joint angles using the orientation of the pose and the known solutions. Our closed-form solution has a significant advantage when implemented as a parallel algorithm on a multi-core processor. The general solution for (2n+1)R is based on the first result by changing the end-effector (use parameters, e.g., joints parameters, to parametrize the position and orientation). One of our main contributions is that we can give a geometric view of the inverse kinematics solutions. By the particular pattern of the circular manipulators, we can pick the special sub-chain with 7R, which is a 7R circular manipulator. We can choose multiple such sub-chains to solve the redundancy with this particular pattern. In addition, we give a conjecture for kinematic singularities of circular manipulators in a formula, which confirms for $n = 5, 6, 7$. The analysis of kinematic singularities shows that they are helpful. Especially, at some singularity, for obstacle avoidance, one has to pass through it instead of avoiding it. From the authors' knowledge, one can not avoid obstacles by keeping away singularities simultaneously using the existing methods, e.g., the null-space method. The symbolic analysis for the kinematic singularity is general and can be applied to any other robot. It is worth mentioning that the robot we treat in this paper is particularly interesting by its geometry. Compared to the null space method, a well-used numeric method in the literature for solving redundancy, we expect to utilize the potential of redundancy more inclusively with our geometric explanation. For example, to avoid obstacles, realize compliance control, or even multi-prioritize configuration variations that take a more inclusive view of possible re-configurations. Some serial manipulators, e.g., ABB Yumi 7R and UFACTORY xArm 7R, are not circular. Because the first or the last three joints fulfill the Bennett conditions (e.g., $a_1 \sin\alpha_2 = a_2 \sin\alpha_1$, $d_2 = 0$) instead of spherical conditions (e.g., $a_1 = a_2 = 0$, $d_2 = 0$). The authors do not know closed-form inverse kinematic solutions for either. We know that the two Bennett conditions reduce the number of solutions from sixteen to eight by Selig's book [32]. The singularities analysis can be done similarly as in Section V, but the representation is more complicated comparing the circular manipulators. We leave all these for future study.

Appendix
Ideals of Kinematic Singularities

$$\begin{aligned} I_5 = \langle & t_2t_4(t_5^2-1), t_2t_4t_6, (t_3^2-1)t_4t_6 \\ & t_2t_4t_7, t_2t_4t_8, (t_3^2-1)t_4t_7, (t_3^2-1)t_4t_8, t_2t_6(t_7^2-1), \\ & t_3t_6(t_7^2-1), t_2t_6t_8, t_3t_6t_8, t_4t_6(t_7^2-1), t_4t_6t_8, (t_5^2-1)t_6t_8 \\ & t_2t_4t_9, t_2t_4t_{10}, t_2t_6t_9, t_2t_6t_{10}, t_3t_6t_9, t_3t_6t_{10}, t_2t_8t_{10}, t_3t_8t_{10}, \\ & t_2t_8(t_9^2-1), (t_3^2-1)t_4t_9, (t_3^2-1)t_4t_{10}, t_3t_8(t_9^2-1), \\ & t_4t_6t_9, (t_5^2-1)t_6t_9, (t_5^2-1)t_6t_{10}, t_4t_8(t_9^2-1), t_5t_8(t_9^2-1), \\ & t_4t_6t_{10}, t_4t_8t_{10}, t_5t_8t_{10}, t_6t_8(t_9^2-1), t_6t_8t_{10}, (t_7^2-1)t_8t_{10} \rangle. \end{aligned}$$

$$I_6 = \langle I_5,$$
$$t_2t_4t_{11}, t_2t_4t_{12}, t_2t_6t_{11}, t_2t_6t_{12}, t_3t_6t_{11}, t_3t_6t_{12},$$
$$t_2t_8t_{11}, t_2t_8t_{12}, t_3t_8t_{11}, t_3t_8t_{12}, t_2t_{10}t_{12}, t_3t_{10}t_{12},$$
$$t_2t_{10}(t_{11}^2-1), t_3t_{10}(t_{11}^2-1), (t_3^2-1)t_4t_{11}, (t_3^2-1)t_4t_{12},$$
$$t_4t_6t_{11}, t_4t_6t_{12}, t_4t_8t_{11}, t_4t_8t_{12}, t_5t_8t_{11}, t_5t_8t_{12},$$
$$t_4t_{10}t_{12}, t_4t_{10}(t_{11}^2-1), t_5t_{10}t_{12}, (t_5^2-1)t_6t_{11},$$
$$(t_5^2-1)t_6t_{12}, t_5t_{10}(t_{11}^2-1), t_6t_8t_{11}, t_6t_8t_{12}, (t_9^2-1)t_{10}t_{12},$$
$$(t_7^2-1)t_8t_{11}, (t_7^2-1)t_8t_{12}, t_6t_{10}(t_{11}^2-1), t_7t_{10}(t_{11}^2-1),$$
$$t_6t_{10}t_{12}, t_7t_{10}t_{12}, t_8t_{10}(t_{11}^2-1), t_8t_{10}t_{12}\rangle.$$

$$I_7 = \langle I_6,$$
$$t_2t_4t_{13}, t_2t_4t_{14}, t_2t_6t_{13}, t_2t_6t_{14}, t_3t_6t_{13}, t_3t_6t_{14},$$
$$t_2t_8t_{13}, t_2t_8t_{14}, t_3t_8t_{13}, t_3t_8t_{14}, t_2t_{10}t_{13}, t_3t_{10}t_{13},$$
$$t_2t_{10}t_{14}, t_3t_{10}t_{14}, t_2t_{12}t_{14}, t_3t_{12}t_{14}, t_2t_{12}(t_{13}^2-1),$$
$$t_3t_{12}(t_{13}^2-1), (t_3^2-1)t_4t_{13}, (t_3^2-1)t_4t_{14},$$
$$t_4t_6t_{13}, t_4t_6t_{14}, t_4t_8t_{13}, t_4t_8t_{14}, t_5t_8t_{13}, t_5t_8t_{14},$$
$$t_4t_{10}t_{13}, t_4t_{10}t_{14}, t_5t_{10}t_{13}, t_5t_{10}t_{14}, t_4t_{12}t_{14}, t_5t_{12}t_{14},$$
$$t_4t_{12}(t_{13}^2-1), t_5t_{12}(t_{13}^2-1), (t_5^2-1)t_6t_{13},$$
$$(t_5^2-1)t_6t_{14}, t_6t_8t_{13}, t_6t_8t_{14}, t_6t_{10}t_{13}, t_6t_{10}t_{14},$$
$$t_7t_{10}t_{13}, t_7t_{10}t_{14}, t_6t_{12}t_{14}, t_5t_{12}t_{14}, t_6t_{12}(t_{13}^2-1),$$
$$(t_7^2-1)t_8t_{13}, (t_7^2-1)t_8t_{14}, t_7t_{12}(t_{13}^2-1),$$
$$t_8t_{10}t_{13}, t_8t_{10}t_{14}, t_{10}t_{13}(t_9^2-1), (t_9^2-1)t_{10}t_{14},$$
$$t_8t_{12}(t_{13}^2-1), t_9t_{12}(t_{13}^2-1), t_8t_{12}t_{14}, t_9t_{12}t_{14},$$
$$t_{10}t_{12}(t_{13}^2-1), t_{10}t_{12}t_{14}, (t_{11}^2-1)t_{12}t_{14}\rangle.$$

Recall that the prime decomposition of I_3 has 6 components (all are hyperplanes):

$$\langle t_4\rangle, \langle t_2, t_6\rangle, \langle t_2, t_3 \pm 1\rangle, \langle t_6, t_5 \pm 1\rangle.$$

The prime decomposition of I_4 has 15 hyperplanes:

$$\langle t_4, t_6\rangle, \langle t_2, t_3 \pm 1, t_6\rangle, \langle t_4, t_7 \pm 1, t_8\rangle,$$
$$\langle t_2, t_3 \pm 1, t_7 \pm 1, t_8\rangle, \langle t_2, t_3, t_4, t_5 \pm 1\rangle,$$
$$\langle t_8, t_7, t_6, t_5 \pm 1\rangle, \langle t_2, t_3, t_4, t_8\rangle, \langle t_2, t_6, t_7, t_8\rangle.$$

The prime decomposition of I_5 has 28 hyperplanes:

$$\langle t_4, t_6, t_8\rangle, \langle t_4, t_6, t_9 \pm 1, t_{10}\rangle, \langle t_2, t_3 \pm 1, t_6, t_8\rangle,$$
$$\langle t_2, t_3 \pm 1, t_6, t_9 \pm 1, t_{10}\rangle, \langle t_4, t_7 \pm 1, t_8, t_9, t_{10}\rangle,$$
$$\langle t_8, t_5 \pm 1, t_4, t_3, t_2\rangle, \langle t_{10}, t_9 \pm 1, t_5 \pm 1, t_4, t_3, t_2\rangle,$$
$$\langle t_2, t_3 \pm 1, t_7 \pm 1, t_8, t_9, t_{10}\rangle, \langle t_5 \pm 1, t_6, t_7, t_8, t_9, t_{10}\rangle,$$
$$\langle t_2, t_6, t_7, t_8, t_9, t_{10}\rangle, \langle t_2, t_3, t_4, t_8, t_9, t_{10}\rangle,$$
$$\langle t_{10}, t_6, t_5, t_4, t_3, t_2\rangle, \langle t_2, t_3, t_4, t_5, t_6, t_7 \pm 1\rangle.$$

The prime decomposition of I_6 has 45 hyperplanes:

$$\langle t_4, t_6, t_8, t_{10}\rangle, \langle t_4, t_6, t_8, t_{11} \pm 1, t_{12}\rangle, \langle t_{10}, t_8, t_6, t_3 \pm 1, t_2\rangle,$$
$$\langle t_{12}, t_{11} \pm 1, t_8, t_6, t_3 \pm 1, t_2\rangle, \langle t_4, t_6, t_9 \pm 1, t_{10}, t_{11}, t_{12}\rangle,$$
$$\langle t_{10}, t_8, t_5 \pm 1, t_4, t_3, t_2\rangle, \langle t_{12}, t_{11} \pm 1, t_8, t_5 \pm 1, t_4, t_3, t_2\rangle,$$
$$\langle t_2, t_3 \pm 1, t_6, t_9 \pm 1, t_{10}, t_{11}, t_{12}\rangle,$$
$$\langle t_{12}, t_{11}, t_{10}, t_9, t_8, t_7 \pm 1, t_4\rangle, \langle t_2, t_3, t_4, t_5, t_6, t_7 \pm 1, t_{10}\rangle,$$
$$\langle t_2, t_3, t_4, t_5, t_6, t_7 \pm 1, t_{11} \pm 1, t_{12}\rangle,$$
$$\langle t_2, t_3, t_4, t_5 \pm 1, t_9 \pm 1, t_{10}, t_{11}, t_{12}\rangle,$$
$$\langle t_2, t_3 \pm 1, t_7 \pm 1, t_8, t_9, t_{10}, t_{11}, t_{12}\rangle,$$
$$\langle t_5 \pm 1, t_6, t_7, t_8, t_9, t_{10}, t_{11}, t_{12}\rangle, \langle t_{12}, t_8, t_7, t_6, t_5, t_4, t_3, t_2\rangle,$$
$$\langle t_2, t_6, t_7, t_8, t_9, t_{10}, t_{11}, t_{12}\rangle, \langle t_2, t_3, t_4, t_8, t_9, t_{10}, t_{11}, t_{12}\rangle,$$
$$\langle t_{12}, t_{11}, t_{10}, t_6, t_5, t_4, t_3, t_2\rangle, \langle t_2, t_3, t_4, t_5, t_6, t_7, t_8, t_9 \pm 1\rangle.$$

The prime decomposition of I_7 has 66 hyperplanes:

$$\langle t_4, t_6, t_8, t_{10}, t_{12}\rangle, \langle t_4, t_6, t_8, t_{10}, t_{13} \pm 1, t_{14}\rangle,$$
$$\langle t_{12}, t_{10}, t_8, t_6, t_3 \pm 1, t_2\rangle,$$
$$\langle t_{14}, t_{13} \pm 1, t_{10}, t_8, t_6, t_3 \pm 1, t_2\rangle,$$
$$\langle t_4, t_6, t_8, t_{11} \pm 1, t_{12}, t_{13}, t_{14}\rangle,$$
$$\langle t_{12}, t_{10}, t_8, t_5 \pm 1, t_4, t_3, t_2\rangle,$$
$$\langle t_{14}, t_{13} \pm 1, t_{10}, t_8, t_5 \pm 1, t_4, t_3, t_2\rangle,$$
$$\langle t_2, t_3 \pm 1, t_6, t_8, t_{11} \pm 1, t_{12}, t_{13}, t_{14}\rangle,$$
$$\langle t_4, t_6, t_9 \pm 1, t_{10}, t_{11}, t_{12}, t_{13}, t_{14}\rangle,$$
$$\langle t_{12}, t_{10}, t_7 \pm 1, t_6, t_5, t_4, t_3, t_2\rangle,$$
$$\langle t_{14}, t_{13} \pm 1, t_{10}, t_7 \pm 1, t_6, t_5, t_4, t_3, t_2\rangle,$$
$$\langle t_{14}, t_{13}, t_{12}, t_{11} \pm 1, t_8, t_5 \pm 1, t_4, t_3, t_2\rangle,$$
$$\langle t_2, t_3 \pm 1, t_6, t_9 \pm 1, t_{10}, t_{11}, t_{12}, t_{13}, t_{14}\rangle,$$
$$\langle t_4, t_7 \pm 1, t_8, t_9, t_{10}, t_{11}, t_{12}, t_{13}, t_{14}\rangle,$$
$$\langle t_{12}, t_9 \pm 1, t_8, t_7, t_6, t_5, t_4, t_3, t_2\rangle,$$
$$\langle t_{14}, t_{13} \pm 1, t_9 \pm 1, t_8, t_7, t_6, t_5, t_4, t_3, t_2\rangle,$$
$$\langle t_{14}, t_{13}, t_{12}, t_{11} \pm 1, t_7 \pm 1, t_6, t_5, t_4, t_3, t_2\rangle,$$
$$\langle t_2, t_3, t_4, t_5 \pm 1, t_9 \pm 1, t_{10}, t_{11}, t_{12}, t_{13}, t_{14}\rangle,$$
$$\langle t_2, t_3 \pm 1, t_7 \pm 1, t_8, t_9, t_{10}, t_{11}, t_{12}, t_{13}, t_{14}\rangle,$$
$$\langle t_5 \pm 1, t_6, t_7, t_8, t_9, t_{10}, t_{11}, t_{12}, t_{13}, t_{14}\rangle,$$
$$\langle t_2, t_6, t_7, t_8, t_9, t_{10}, t_{11}, t_{12}, t_{13}, t_{14}\rangle,$$
$$\langle t_2, t_3, t_4, t_8, t_9, t_{10}, t_{11}, t_{12}, t_{13}, t_{14}\rangle,$$
$$\langle t_2, t_3, t_4, t_5, t_6, t_{10}, t_{11}, t_{12}, t_{13}, t_{14}\rangle,$$
$$\langle t_2, t_3, t_4, t_5, t_6, t_7, t_8, t_{12}, t_{13}, t_{14}\rangle,$$
$$\langle t_2, t_3, t_4, t_5, t_6, t_7, t_8, t_9, t_{10}, t_{14}\rangle,$$
$$\langle t_2, t_3, t_4, t_5, t_6, t_7, t_8, t_9, t_{10}, t_{11} \pm 1\rangle.$$

References

[1] Y. Wang and P. Artemiadis, "Closed-form inverse kinematic solution for anthropomorphic motion in redundant robot arms," *Advances in Robotics & Automation*, vol. 2, no. 110, p. 2, 2013.

[2] M. Brandstötter, A. Angerer, and M. Hofbaur, "An analytical solution of the inverse kinematics problem of industrial serial manipulators with an ortho-parallel basis and a spherical wrist," in *Proceedings of the Austrian Robotics Workshop*, 2014, pp. 7–11.

[3] S. Kim, C. Kim, and J. H. Park, "Human-like arm motion generation for humanoid robots using motion capture database," in *2006 IEEE/RSJ International Conference on Intelligent Robots and Systems*. IEEE, 2006, pp. 3486–3491.

[4] J. F. Soechting and M. Flanders, "Errors in pointing are due to approximations in sensorimotor transformations," *Journal of neurophysiology*, vol. 62, no. 2, pp. 595–608, 1989.

[5] M. Pfurner, "Closed form inverse kinematics solution for a redundant anthropomorphic robot arm," *Computer Aided Geometric Design*, vol. 47, pp. 163–171, 2016.

[6] J. F. Soechting and M. Flanders, "Sensorimotor representations for pointing to targets in three-dimensional space," *Journal of Neurophysiology*, vol. 62, no. 2, pp. 582–594, 1989.

[7] J. Denavit and R. S. Hartenberg, "A kinematic notation for lower-pair mechanisms based on matrices." *Trans. of the ASME. Journal of Applied Mechanics*, vol. 22, pp. 215–221, 1955. [Online]. Available: http://ci.nii.ac.jp/naid/10008019314/en/

[8] H. Kim, L. M. Miller, N. Byl, G. M. Abrams, and J. Rosen, "Redundancy resolution of the human arm and an upper limb exoskeleton," *IEEE Transactions on Biomedical Engineering*, vol. 59, no. 6, pp. 1770–1779, 2012.

[9] C. Faria, F. Ferreira, W. Erlhagen, S. Monteiro, and E. Bicho, "Position-based kinematics for 7-dof serial manipulators with global configuration control, joint limit and singularity avoidance," *Mechanism and Machine Theory*, vol. 121, pp. 317–334, 2018.

[10] B. Bongardt, "Inverse kinematics of anthropomorphic arms yielding eight coinciding circles," in *Computational Kinematics*. Springer, 2018, pp. 525–534.

[11] A. Ghosal, "Resolution of redundancy in robots and in a human arm," *Mechanism and Machine Theory*, vol. 125, pp. 126–136, 2018.

[12] A. Liegeois *et al.*, "Automatic supervisory control of the configuration and behavior of multibody mechanisms," *IEEE transactions on systems, man, and cybernetics*, vol. 7, no. 12, pp. 868–871, 1977.

[13] A. A. Maciejewski and C. A. Klein, "Obstacle avoidance for kinematically redundant manipulators in dynamically varying environments," *The international journal of robotics research*, vol. 4, no. 3, pp. 109–117, 1985.

[14] Y. Nakamura, H. Hanafusa, and T. Yoshikawa, "Task-priority based redundancy control of robot manipulators," *The International Journal of Robotics Research*, vol. 6, no. 2, pp. 3–15, 1987.

[15] D. E. Whitney, "Resolved motion rate control of manipulators and human prostheses," *IEEE Transactions on man-machine systems*, vol. 10, no. 2, pp. 47–53, 1969.

[16] J. Hollerbach and K. Suh, "Redundancy resolution of manipulators through torque optimization," *IEEE Journal on Robotics and Automation*, vol. 3, no. 4, pp. 308–316, 1987.

[17] B. Siciliano and J.-J. Slotine, "A general framework for managing multiple tasks in highly redundant robotic systems," in *Fifth International Conference on Advanced Robotics 'Robots in Unstructured Environments*, 1991, pp. 1211–1216 vol.2.

[18] D. Omrčen, L. Žlajpah, and B. Nemec, "Compensation of velocity and/or acceleration joint saturation applied to redundant manipulator," *Robotics and Autonomous Systems*, vol. 55, no. 4, pp. 337–344, 2007.

[19] F. Flacco, A. De Luca, and O. Khatib, "Motion control of redundant robots under joint constraints: Saturation in the null space," in *2012 IEEE International Conference on Robotics and Automation*. IEEE, 2012, pp. 285–292.

[20] Y. Nakamura, *Advanced robotics: redundancy and optimization*. Addison-Wesley Longman Publishing Co., Inc., 1990.

[21] A. Kecskeméthy and M. Hiller, "Automatic closed-form kinematics-solutions for recursive single-loop chains," in *International Design Engineering Technical Conferences and Computers and Information in Engineering Conference*, vol. 9419. American Society of Mechanical Engineers, 1992, pp. 387–393.

[22] A. Müller and D. Zlatanov, *Singular Configurations of Mechanisms and Manipulators*. Springer, 2019, vol. 589.

[23] G. Hegedüs, J. Schicho, and H.-P. Schröcker, "Factorization of rational curves in the Study quadric," *Mechanism and Machine Theory*, vol. 69, pp. 142–152, 2013.

[24] Z. Li, "Closed linkages with six revolute joints," PhD thesis, Johannes Kepler University Linz, 2015.

[25] G. Hegedüs, J. Schicho, and H.-P. Schröcker, "The theory of bonds: A new method for the analysis of linkages," *Mechanism and Machine Theory*, vol. 70, no. 0, pp. 407–424, 2013.

[26] M. L. Husty and H.-P. Schröcker, "Algebraic geometry and kinematics," in *Nonlinear Computational Geometry*, ser. The IMA Volumes in Mathematics and its Applications, I. Z. Emiris, F. Sottile, and T. Theobald, Eds. Springer, 2010, vol. 151, ch. Algebraic Geometry and Kinematics, pp. 85–107.

[27] M. Brandstötter, S. Mühlbacher-Karrer, D. Schett, and H. Zangl, "Virtual compliance control of a kinematically redundant serial manipulator with 9 dof," in *International Conference on Robotics in Alpe-Adria Danube Region*. Springer, 2016, pp. 38–46.

[28] J. E. Baker, "Displacement–closure equations of the unspecialised double-hooke's-joint linkage," *Mechanism and machine Theory*, vol. 37, no. 10, pp. 1127–1144, 2002.

[29] M. J. D. Hayes, H. Husty, and P. J. Zsombor-Murray, "Singular configurations of wrist-partitioned 6R serial robots: a geometric perspective for users," *Trans. Can. Soc. Mech. Eng.*, vol. 26, pp. 41–56, 2002.

[30] A. Karger, "Singularity analysis of serial robot manipulators," *ASME J. Mech. Des.*, vol. 118, pp. 505–525, 1996.

[31] D. Cox, J. Little, and D. OShea, *Ideals, varieties, and algorithms: an introduction to computational algebraic geometry and commutative algebra*. Springer Science & Business Media, 2013.

[32] J. Selig, *Geometric Fundamentals of Robotics*, 2nd ed., ser. Monographs in Computer Science. Springer, 2005.

Zijia Li received a Ph.D. in natural sciences from Johannes Kepler Universität Linz in 2016. He holds the position of associated researcher at the KLMM in the Academy of Mathematics and Systems Science (AMSS) of the Chinese Academy of Sciences (CAS). His research focuses primarily on symbolic computation, computational kinematics, and singularities.

Mathias Brandstötter (Member, IEEE) received the Ph.D. degree in technical sciences from UMIT, Private University of Health Sciences and Technology, in 2016. He actually holds the position of Deputy Director at the Institute of Robotics and Mechatronics at JOANNEUM RESEARCH Forschungsgesellschaft. He is developing and leading interdisciplinary research projects since working with JOANNEUM RESEARCH and is author and co-author of several journal and conference papers in the area of robotics. His research focuses primarily on collaborative robotics, mobile manipulation, robot kinematics and robot safety.

Michael Hofbaur (Member, IEEE) is Director and Chief Scientist of JOANNEUM RESEARCH ROBOTICS and Professor for Modular Robotics at the Alpen-Adria University Klagenfurt. Prior to these roles, he was Professor of Automation and Control at the private university UMIT in Hall/Tyrol, Visiting Professor at the Space Systems Laboratory and the AI Laboratory of M.I.T. in Cambridge USA, and University Lecturer at the Graz University of Technology. In addition to his scientific career path, he became a Chartered Engineer in Electrical Engineering and worked as consultant for Systems Engineering and Functional Safety. His research focusses on innovative industrial and service robotics and human-robot interaction that builds upon model-based and systems theoretic methodologies for the control and AI based concepts for systems diagnosis, planning and intelligent control. Work on functional- and robot safety support his focus on building safety-rated control concepts for modern robot systems.